



HAL
open science

Strigolactone signalling inhibits trehalose 6-phosphate signalling independently of BRC1 to suppress shoot branching

Franziska Fichtner, Jazmine L Humphreys, Francois F Barbier, Regina Feil, Philipp Westhoff, Anna Moseler, John E Lunn, Steven M Smith, Christine A Beveridge

► To cite this version:

Franziska Fichtner, Jazmine L Humphreys, Francois F Barbier, Regina Feil, Philipp Westhoff, et al.. Strigolactone signalling inhibits trehalose 6-phosphate signalling independently of BRC1 to suppress shoot branching. *New Phytologist*, 2024, 244 (3), pp.900-913. 10.1111/nph.20072 . hal-04690214

HAL Id: hal-04690214

<https://hal.inrae.fr/hal-04690214v1>

Submitted on 6 Sep 2024










HAL is a multi-disciplinary open access archive for the deposit and dissemination of scientific research documents, whether they are published or not. The documents may come from teaching and research institutions in France or abroad, or from public or private research centers.

L'archive ouverte pluridisciplinaire **HAL**, est destinée au dépôt et à la diffusion de documents scientifiques de niveau recherche, publiés ou non, émanant des établissements d'enseignement et de recherche français ou étrangers, des laboratoires publics ou privés.



Distributed under a Creative Commons Attribution - NonCommercial - NoDerivatives 4.0 International License

Strigolactone signalling inhibits trehalose 6-phosphate signalling independently of BRC1 to suppress shoot branching

Franziska Fichtner^{1,2,3,4,5} , Jazmine L. Humphreys^{6*} , Francois F. Barbier^{1,2,7*} , Regina Feil⁵ , Philipp Westhoff⁴ , Anna Moseler⁸ , John E. Lunn⁵ , Steven M. Smith⁶  and Christine A. Beveridge^{1,2} 

¹School of Agriculture and Food Sustainability, The University of Queensland, St Lucia, QLD, 4072, Australia; ²ARC Centre for Plant Success in Nature and Agriculture, The University of Queensland, St Lucia, QLD, 4072, Australia; ³Faculty of Mathematics and Natural Sciences, Institute of Plant Biochemistry, Heinrich Heine University Düsseldorf, Düsseldorf, 40225, Germany; ⁴Cluster of Excellence in Plant Science (CEPLAS), Heinrich Heine University, Düsseldorf, 40225, Germany; ⁵Max Planck Institute of Molecular Plant Physiology, Potsdam-Golm, 14476, Germany; ⁶ARC Centre for Plant Success in Nature and Agriculture, School of Natural Sciences, University of Tasmania, Hobart, TAS, 7001, Australia; ⁷Institute for Plant Sciences of Montpellier, University of Montpellier, CNRS, INRAE, Institut Agro, Montpellier, 34060, France; ⁸INRES-Chemical Signalling, University of Bonn, Bonn, 53113, Germany

Summary

Authors for correspondence:

Franziska Fichtner

Email: franziska.fichtner@hhu.de

Christine A. Beveridge

Email: c.beveridge@uq.edu.au

Received: 10 April 2024

Accepted: 3 August 2024

New Phytologist (2024)

doi: 10.1111/nph.20072

Key words: *Arabidopsis thaliana*, garden pea, plant architecture, shoot branching, strigolactone, sugar signalling, trehalose 6-phosphate.

- The phytohormone strigolactone (SL) inhibits shoot branching, whereas the signalling metabolite trehalose 6-phosphate (Tre6P) promotes branching. How Tre6P and SL signalling may interact and which molecular mechanisms might be involved remains largely unknown.
- Transcript profiling of *Arabidopsis* SL mutants revealed a cluster of differentially expressed genes highly enriched in the Tre6P pathway compared with wild-type (WT) plants or *brc1* mutants. Tre6P-related genes were also differentially expressed in axillary buds of garden pea (*Pisum sativum*) SL mutants.
- Tre6P levels were elevated in the SL signalling mutant *more axillary (max) growth 2* compared with other SL mutants or WT plants indicating a role of MAX2-dependent SL signalling in regulating Tre6P levels.
- A transgenic approach to increase Tre6P levels demonstrated that all SL mutant lines and *brc1* flowered earlier, showing all of these mutants were responsive to Tre6P. Elevated Tre6P led to increased branching in WT plants but not in *max2* and *max4* mutants, indicating some dependency between the SL pathway and Tre6P regulation of shoot branching. By contrast, elevated Tre6P led to an enhanced branching phenotype in *brc1* mutants indicating independence between BRC1 and Tre6P. A model is proposed whereby SL signalling represses branching via Tre6P and independently of the BRC1 pathway.

Introduction

Shoot branching is a complex developmental process by which new shoots emerge from suppressed axillary buds located in leaf axils. The shoot tip suppresses branching by acting as a source of the plant hormone auxin (Domagalska & Leyser, 2011; Barbier *et al.*, 2019b) and as a sink for photoassimilates (Mason *et al.*, 2014). Auxin produced by the growing shoot tip travels basipetally towards the root and inhibits bud outgrowth. Auxin is thought to act partly through inhibiting the synthesis of cytokinins, which activate bud outgrowth, and partly via stimulating synthesis of strigolactones (SLs), which inhibit bud outgrowth (Barbier *et al.*, 2019b). SL signalling is mediated by DWARF14 (D14), an α/β -fold hydrolase that binds SLs (Arite *et al.*, 2009; Hamiaux *et al.*, 2012). Upon perception of SL, D14 binds to the F-box protein MORE AXILLARY GROWTH2 (MAX2), which

is part of an SCF (SKP, Cullin, F-box) complex (Stirnberg *et al.*, 2007). Upon D14 binding, SCF_{MAX2} targets SUPPRESSOR OF MAX2-LIKE 6, 7 and 8 (SMXL6,7,8) proteins, which are activators of branching, for polyubiquitination and degradation via the 26S proteasome (Jiang *et al.*, 2013; Soundappan *et al.*, 2015; Wang *et al.*, 2015). One known target of SMXL proteins is *BRC1*, encoding a transcription factor that inhibits branching (Aguilar-Martínez *et al.*, 2007; Wang *et al.*, 2020). As *brc1* mutants do not branch as substantially as SL mutants, it has been suggested that, notwithstanding redundancy, SL acts via an additional BRC1 independent pathway(s) (Seale *et al.*, 2017; Luo *et al.*, 2021).

Auxin also inhibits shoot branching by inhibiting the auxin export of buds into the main auxin transport stream. In this model, axillary bud outgrowth requires that axillary buds establish their own polar auxin transport stream to export auxin into the main stem which, in turn, promotes their sustained growth and regulates the outgrowth of other axillary buds (Prusinkiewicz

*These authors contributed equally to this work.

et al., 2009; Domagalska & Leyser, 2011). In this model, SLs mainly act by modulating the ease with which the polar auxin transport can be established in each bud, by either increasing (low SLs) or decreasing (high SLs) auxin transporter accumulation at the plasma membrane (Bennett *et al.*, 2006; Crawford *et al.*, 2010; Shinohara *et al.*, 2013). *MAX1*, *MAX2*, *D14* and *SMXL* genes are highly expressed in the vasculature (xylem and phloem as well as parenchyma cells) (Booker *et al.*, 2005; Stirnberg *et al.*, 2007; Chevalier *et al.*, 2014; Soundappan *et al.*, 2015). The expression of these genes in the xylem parenchyma cells is consistent with the auxin canalisation model. Given that the phloem transports and delivers many compounds involved in growth and development, including sugars, it is possible that the vascular localisation of several SL genes has importance in addition to mediating auxin transport.

Several studies have now demonstrated that, after decapitation of the shoot apex, auxin levels in the lower parts of the shoot do not correspond well with the initial bud outgrowth response, which is often referred to as bud release (Morris *et al.*, 2005; Mason *et al.*, 2014; Cao *et al.*, 2023). It has been suggested that auxin canalisation is more important in later stages of bud outgrowth and for the competition between buds (Bennett *et al.*, 2016a; Barbier *et al.*, 2019b; Cao *et al.*, 2023), whereas sugar availability to the buds has emerged as a key player in mediating bud release (Mason *et al.*, 2014; Barbier *et al.*, 2015; Fichtner *et al.*, 2017). In this model, the growing shoot tip suppresses axillary bud outgrowth through its strong sink strength, which deprives axillary buds of sugars (Mason *et al.*, 2014; Barbier *et al.*, 2019b). Sugars can be sensed by different signalling systems thus allowing plants to adjust their metabolism, growth and development to specific environmental conditions (Fichtner *et al.*, 2021b). Accordingly, it has now been demonstrated in numerous studies that sugar availability is a key regulator of bud release (Barbier *et al.*, 2019b) and that sugars interact with phytohormone signalling pathways to regulate bud outgrowth (Barbier *et al.*, 2015, 2021; Bertheloot *et al.*, 2020; Salam *et al.*, 2021; Cao *et al.*, 2023). Notably, sucrose was shown to alleviate the inhibitory effect of SLs on bud outgrowth by transcriptional regulation of *MAX2* (Barbier *et al.*, 2015; Bertheloot *et al.*, 2020; Patil *et al.*, 2022). Sucrose was also suggested to increase cytokinin levels to trigger bud release (Cao *et al.*, 2023).

Trehalose 6-phosphate (Tre6P) is a signal of sucrose availability in plants (Lunn *et al.*, 2006; Fichtner & Lunn, 2021). Tre6P levels increase very early after decapitation of the shoot apex and this increase corresponds to the increase in bud size (Fichtner *et al.*, 2017). We later confirmed a local role of Tre6P in the regulation of axillary bud outgrowth by lowering Tre6P specifically in axillary buds in *Arabidopsis*. Transgenic lines with lower levels of Tre6P in the buds showed a strong delay in bud release (Fichtner *et al.*, 2021a). In addition, Tre6P also modulated branching in a systemic manner as lines with an increase in Tre6P in the vasculature had more branches (Fichtner *et al.*, 2021a). It is likely that increased levels of Tre6P in the vasculature promote branching through enhanced sucrose allocation towards the buds and through transcriptional activation of *FLOWERING LOCUS T*

(Fichtner *et al.*, 2021a). The interaction between Tre6P and phytohormones is poorly understood.

There is evidence that *MAX2* activity is inhibited by citrate, an intermediate of the tricarboxylic acid (TCA) cycle (Tal *et al.*, 2022). A transient increase in Tre6P was shown to increase citrate levels, by activating the anaplerotic flux of carbon into the TCA cycle to stimulate organic acid and amino acid synthesis (Figuroa *et al.*, 2016). This is again consistent with the location of SL and Tre6P synthesis and signalling in the phloem.

Here, we elucidated a connection between sugar signalling via Tre6P and SL signalling in the control of shoot branching. We identified the Tre6P pathway as a new downstream target of SL signalling using an RNA sequencing (RNA-seq) approach. We showed that Tre6P synthesis is activated in SL mutants and regulators of Tre6P signalling are also transcriptionally altered. Using a genetic approach, we demonstrated that increasing Tre6P in the vasculature increased branching in *brc1* mutants but did not increase branching in SL mutants. Decreasing Tre6P in *max2* plants inhibited and strongly delayed branching.

Materials and Methods

Plant material and growth

Arabidopsis thaliana (L.) Heynh. accession Columbia-0 (Col-0) accessions and mutants in this background were used. *Arabidopsis* seeds were placed on agar plates containing 1/2-strength Murashige & Skoog medium (1/2 MS), stratified for 72 h at 4°C in the dark and then moved to a growth chamber. After 7 d in the light, single plants were transferred to 6-cm diameter pots. LED lights with an irradiance of either 75 or 150 $\mu\text{mol m}^{-2} \text{s}^{-1}$ (higher light intensity, also used for short-day experiment), and 16-h photoperiods (8-h photoperiod for short-day experiment), and a temperature of 22°C : 18°C, day : night were used. *Arabidopsis* lines in the Col-0 background were those described in the accompanying references: *brc1-2* (Aguilar-Martínez *et al.*, 2007), *max2-1* (Stirnberg *et al.*, 2002), *max4-1* (Sorefan *et al.*, 2003), *d14-1* (Chevalier *et al.*, 2014), *kai2-2* (Waters *et al.*, 2015), *smxl6,7,8* (*-smxl6-4,7-3,8-1*) (Soundappan *et al.*, 2015), *pGLDPA:otsA* (Line 1) (Fichtner *et al.*, 2021a) and *pGLDPA:CeTPP* (Line 4) (Fichtner *et al.*, 2021a). Double and quadruple mutants were generated in this study by crossing of the respective parental lines. *Pisum sativum* cv. Torsdag (L107) wild-type (WT), *ramosus1-2* (*rms1-2T*) or *rms4-1* (K164) mutants (Beveridge *et al.*, 1997a,b) in the L107 background were used and grown in a 16-h photoperiod, with an irradiance of 200 to 300 $\mu\text{mol m}^{-2} \text{s}^{-1}$ and 25°C : 20°C, day : night temperatures.

RNA-seq pre-data processing and differential gene expression analysis

Five biological replicates per genotype were used to prepare libraries (total $10 \times 5 = 50$ libraries) for each sample by Illumina Stranded mRNA library prep (Illumina, San Diego, CA, USA; www.illumina.com). RNA was extracted using the ISOLATE II RNA Mini Kit (Bioline, Memphis, TN, USA; www.illumina.com).

bioline.com). Total RNA was quantified using a Qubit fluorimeter (Thermo Fisher Scientific, Waltham, MA, USA; www.thermofisher.com), and 2 µg of total RNA was sequenced at the Ramaciotti Centre for Genomics, Sydney, Australia (www.ramaciotti.unsw.edu.au). Paired end read libraries were generated using NovaSeq 6000 S2 2×100bp (each resulting library had over 40 million read pairs). The raw RNA-seq data described in this study have been deposited in the NCBI Short Read Archive (SRA) database under <http://www.ncbi.nlm.nih.gov/bioproject/934161> (Submission ID: SUB12863317, BioProject ID: PRJNA934161). The sequencing data were uploaded to the Galaxy web platform (Afgan *et al.*, 2016), and the public server at usegalaxy.org was used for the following steps: Quality control was carried out using FASTQC, adapter sequences were removed before trimming and filtering by TRIMMOMATIC (Andrews, 2010), and read counts were generated for each transcript/gene by Salmon (Patro *et al.*, 2017) (all libraries had > 90% mapping percentage using the Araport 11 genome annotation, Cheng *et al.* (2017)). Read counts generated by Salmon were then downloaded and used as input for the R package DESEQ2. First, differential gene expression analysis was performed using DESEQ2 v.1.18.1 using a pairwise design formula (Love *et al.*, 2014). DESEQ2 normalises and removes low counts internally. A complete list of DEGs for each mutant compared with the WT along with the fold change, and adjusted *P*-values is available in Supporting Information Tables S1–S3.

K-means clustering

Reads were normalised using DESEQ2's median of ratios to normalise the depth effect of each library and gene size. The normalised expression matrix was scaled to a Z-scale matrix, and the k-means function in Rstudio Desktop (www.posit.co) was used to cluster genes with the following parameters (set.seed(200 000), centres = *n*, iter.max = 30). Plots were generated with the R packages GGLOT2, DPLYR, TIDYR and PHEATMAP (www.cran.r-project.org).

Gene Ontology term overrepresentation

Gene Ontology (GO) term enrichment was performed using the clueGO cystoscope plugin (Bindea *et al.*, 2009), identifying enriched GO terms with adjusted *P*-values of < 0.05. A minimum of three genes per cluster was required for enrichment to be called.

Phylogenetic analyses

TREHALOSE-6-PHOSPHATE SYNTHASE (TPS) and *TREHALOSE-6-PHOSPHATE PHOSPHATASE* (TPP) homologues in pea were identified by BLASTP analysis of *Arabidopsis thaliana* TPS and TPP sequences against the pea genome (<https://urgi.versailles.inra.fr/blast/>) (Kreplak *et al.*, 2019). Identified TPS and TPP sequences were aligned separately using the global alignment tool (cost matrix Blosum80, gap open penalty 15, gap extension penalty 5, refine iterations 20) using geneious

(<https://www.geneious.com/>). Two consensus trees, one for TPS and one for TPP, were constructed based on Bayesian methods (MR BAYES 3.2.6 (Huelsenbeck & Ronquist, 2001) plugin for geneious with otsA (TPS) or otsB (TPP) as outgroups, otherwise standard parameters) and maximum likelihood (PHYML (Guindon *et al.*, 2010) plugin for geneious with Blosum 62 as substitution model and 100 bootstrap replicates). Only clades with bootstrap values and posterior probabilities of > 65% are shown.

Phenotyping

Primary rosette branches (R1) (shoots/inflorescences ≥ 0.5 cm) that were initiated in the axils of rosette leaves (RL) were counted and RL number was determined as a measure of flowering time and to normalise primary rosette branch by leaf number (R1 : RL).

Metabolite extraction and measurements

Arabidopsis whole rosettes with a visible floral bud in the centre of the rosette (*c.* 2 to 3 d before bolting), or single pea buds (node 4) from 11-d-old pea plants were harvested 10 h after dawn (zeitgeber time, ZT 10). For the short-day experiment, whole *Arabidopsis* rosettes were harvested at the end of the day (ZT 8). All plant tissue was rapidly quenched in liquid nitrogen under ambient growth conditions and frozen plant tissue was ground to a fine powder at liquid nitrogen temperature. Water-soluble metabolites were extracted as described previously (Lunn *et al.*, 2006). Tre6P, other phosphorylated intermediates and organic acids, were measured by anion-exchange high-performance liquid chromatography (HPLC) coupled to tandem mass spectrometry (Lunn *et al.*, 2006; Figueroa *et al.*, 2016). Sucrose was measured enzymatically (Stitt *et al.*, 1989).

qRT-PCR analysis in garden pea

Single pea buds (node 4) from 11-d-old pea plants were harvested at ZT 10. Five single-bud biological replicates from separate plants were harvested per genotype. RNA was extracted from single buds using a CTAB/PVP-based extraction method without phenol or chloroform (Barbier *et al.*, 2019a). Reverse transcription was performed using iScript cDNA synthesis kit (cat no.: 170-8891; Bio-Rad). The polymerase chain reaction mix was prepared using sensiFAST SYBR No-ROX Kit (cat no.: BIO-98050; Meridian Bioscience, Memphis, TN, USA; www.bioline.com), and quantitative reverse transcription polymerase chain reaction was performed using the Qiagen Rotor-gene Q HRM system. Gene expression was calculated using the $\Delta\Delta C_t$ method adjusted for polymerase chain reaction efficiency. The geomean of *P5TUBULIN2*, *P318S* and *P3EF1a* reference genes was used for normalisation. All primers are listed in Table S4.

Statistical analysis and data visualisation

Data analyses and plotting were performed using Rstudio Desktop (www.posit.co) and the packages GGLOT2, STATS and

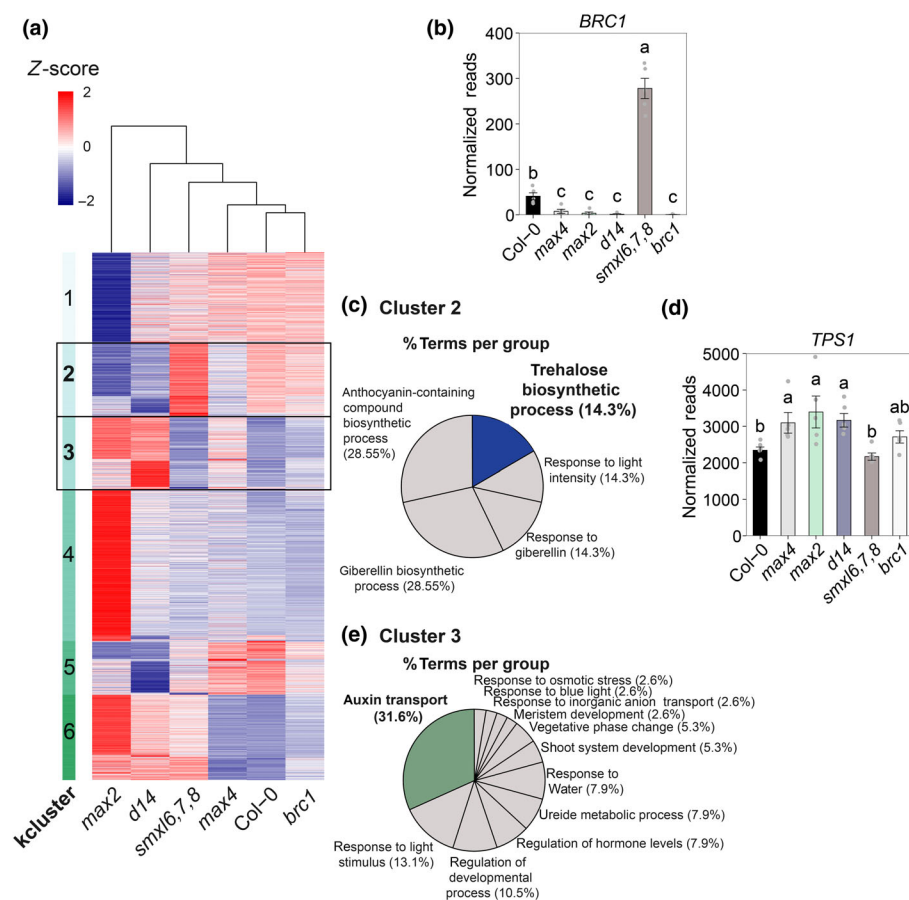


Fig. 1 Transcriptional analysis of strigolactone mutants reveals a connection to sugar signalling via trehalose 6-phosphate. (a) K-means clustering of Z-scores of the means of whole *Arabidopsis thaliana* rosettes, just before bolting, from strigolactone synthesis (*max4*), signalling (*max2*, *d14*) and downstream signalling (*smxl6,7,8* and *brc1*) mutant plants. Hierarchical clustering of the different genotypes is presented by a dendrogram. (b) Normalised RNA-seq reads (derived from DESeq2 analysis) of *BRANCHED1* (*BRC1*) in Arabidopsis wild-type (WT) and mutant plants from (a). (c) Gene Ontology (GO) term enrichment analysis of k-means Cluster 2. Percentages represent % of terms in group. (d) Normalised RNA-seq reads (derived from DESeq2 analysis) of *TREHALOSE-6-PHOSPHATE SYNTHASE1* (*TPS1*) in Arabidopsis WT and mutant plants from (a). (e) GO term enrichment analysis of k-means Cluster 3. Percentages represent % of terms in group. Letters represent significant differences ($P < 0.05$) based on ANOVA with *post hoc* least significant difference (LSD) testing (mean \pm SE, $n = 5$). *brc1*, *branched1*; *d14*, *dwarf14*; *max*, *more axillary growth*; *smxl6,7,8*, *suppressor of max2-like 6, 7 and 8*.

AGRICOLAE (www.cran.r-project.org) using an ANOVA-based *post hoc* comparison of means test (Fisher's least significant difference (LSD) test, significance indicated by letters). Figures were compiled using Adobe Illustrator 2024.

Results

Arabidopsis strigolactone mutants have altered trehalose 6-phosphate synthesis and signalling

SLs are phytohormones with control over many developmental processes (Brewer *et al.*, 2013). Shoot branching is an important and well-studied developmental process that is controlled by SLs. However, our knowledge on SL downstream targets is limited except for the well-established transcription factor *BRC1*, which is transcriptionally repressed by SLs (Lantzouni *et al.*, 2017; Wang *et al.*, 2020; Hellens *et al.*, 2023). Here, we used an RNA-seq approach in a variety of SL mutants to identify new SL targets that are potentially involved in the regulation of shoot branching. We used Arabidopsis mutants deficient in SL synthesis (*max4*), SL signalling (*max2*, *d14*), direct targets of SL signalling (*smxl6,7,8*) and a downstream transcription factor target (*brc1*). Whole Arabidopsis rosettes (shoots) were harvested just before bolting so that they were at the same developmental stage, to avoid artefacts due to differences in development. Clustering analysis of all differentially expressed genes (DEGs) relative to

WT Col-0 plants revealed six distinct clusters (Fig. 1a; Table S1). We then looked for clusters that have DEGs that are either upregulated in *max4*, *max2* and *d14* and downregulated in *smxl6,7,8*, or vice versa. This was the case for two clusters, 2 and 3 (Fig. 1a).

Cluster 2 contained the known target of SLs, *BRC1*, which was downregulated in *max4*, *max2* and *d14*, and strongly upregulated in the *smxl6,7,8* mutant (Fig. 1b), indicating that targets of SLs were represented in this cluster. GO term enrichment of Cluster 2 revealed that 'trehalose biosynthetic process' was highly enriched (14.3%; Fig. 1c). Tre6P is of special interest as it has previously been implicated in triggering axillary bud outgrowth in a local and systemic manner (Fichtner *et al.*, 2017, 2021a). In accordance with Cluster 2 containing branching regulators and potential downstream targets of the SL pathway, the GO terms 'gibberellin biosynthetic process', 'response to gibberellin' and 'anthocyanin-containing compound biosynthetic process' were also significantly enriched (Fig. 1c). Gibberellins have been demonstrated to have a function in the later stages of branch development, rather than in early bud outgrowth, and their levels highly correlate with auxin levels (Cao *et al.*, 2023). Anthocyanin biosynthesis genes have also recently been identified as SL downstream targets in Arabidopsis hypocotyls (Hellens *et al.*, 2023), indicating that Cluster 2 contains downstream targets of the SL pathway.

In accordance with the Tre6P biosynthesis pathway being a target of SLs, we identified *TREHALOSE-6-PHOSPHATE*

SYNTHASE1 (*TPS1*), as being significantly upregulated in *max4*, *max2* and *d14* (Fig. 1d). *TPS1* encodes the main Tre6P synthase and is the predominant, perhaps only, source of Tre6P in Arabidopsis beyond the seed stage (Fichtner *et al.*, 2020). We also analysed the expression of the 10 *TPP* genes in Arabidopsis (Fig. S1). *TPPD* and *TPPF* were both significantly downregulated in *max2* and *d14*, with a similar but nonsignificant trend in *max4* (Fig. S1), but otherwise there was no consistent regulation of *TPP* genes in *max4*, *max2* and *d14*. *TPPF* was also significantly upregulated in the *smxl6,7,8* mutant, with *TPPD* showing the same trend (Fig. S1). These differences in *TPS1* and *TPP* gene expression could potentially be translated into higher levels of Tre6P in SL mutants, via concomitant stimulation of Tre6P synthesis decreased Tre6P dephosphorylation.

TPS1 was part of Cluster 3, which showed the opposite trend to Cluster 2. GO term enrichment of Cluster 3 revealed that 'auxin transport' was the most enriched GO category (31.6%; Fig. 1d). As it is known that auxin transport is altered in SL mutants (Bennett *et al.*, 2006; Crawford *et al.*, 2010; Shinohara *et al.*, 2013; Nahas *et al.*, 2024), this confirms that the harvested material (i.e. whole rosettes at the same developmental stage) and our analysis successfully identified targets of the SL pathway.

In total, there were 41 DEGs in common in the SL mutants *max4*, *max2* and *d14* (Fig. 2a; Table S2), and among these, we found another gene involved in the Tre6P pathway, *TREHALOSE-6-PHOSPHATE SYNTHASE9* (*TPS9*). *TPS9* encodes a catalytically inactive class II TPS protein (Vandesteene *et al.*, 2010; Fichtner & Lunn, 2021). Since class II TPS proteins lack the ability to synthesise Tre6P, it has been speculated that they might serve as Tre6P sensors rather than Tre6P metabolising enzymes (Lunn, 2007; Göbel & Fichtner, 2023). The potential sensor or signalling role of *TPS9* is supported by evidence that it binds to and modulates the activity of the SUCROSE-NON-FERMENTING1-RELATED KINASE1 (SnRK1) *in vitro* (Van Leene *et al.*, 2022). However, how *TPS9* acts *in planta* is unknown. It has also been reported that orthologous class II TPS proteins interact with the OsTPS1 protein in rice, potentially modulating the enzyme's activity (Zang *et al.*, 2011). The *TPS9* transcript is upregulated upon carbon starvation (Ramon *et al.*, 2009). As *TPS9* was significantly downregulated in *max4*, *max2* and *d14*, and upregulated in *smxl6,7,8* (Fig. 2b), this suggests that SL mutants may have a high sugar availability and signalling. Significant downregulation of *TPS9* expression in *max2* and *d14* was also reported in previous studies (Ha *et al.*, 2014; Li *et al.*, 2020) consistent with our results. This pattern of expression suggests that Tre6P levels, especially signalling, are altered in SL mutants.

Endogenous Tre6P levels were measured to test whether they are affected by defects in SL biosynthesis or signalling. Strikingly, Tre6P levels were twice as high in rosettes of the *max2* mutant than in WT plants (Fig. 2c). Sucrose and the Tre6P : sucrose ratio, which is a proxy for the influence Tre6P has on sugar metabolism (Yadav *et al.*, 2014), were also increased in *max2*, while sucrose was decreased in *smxl6,7,8* (Fig. S2a). In parallel, *SWEET11* and *SWEET12*, encoding members of the SUGARS WILL EVENTUALLY BE EXPORTED TRANSPORTER family responsible

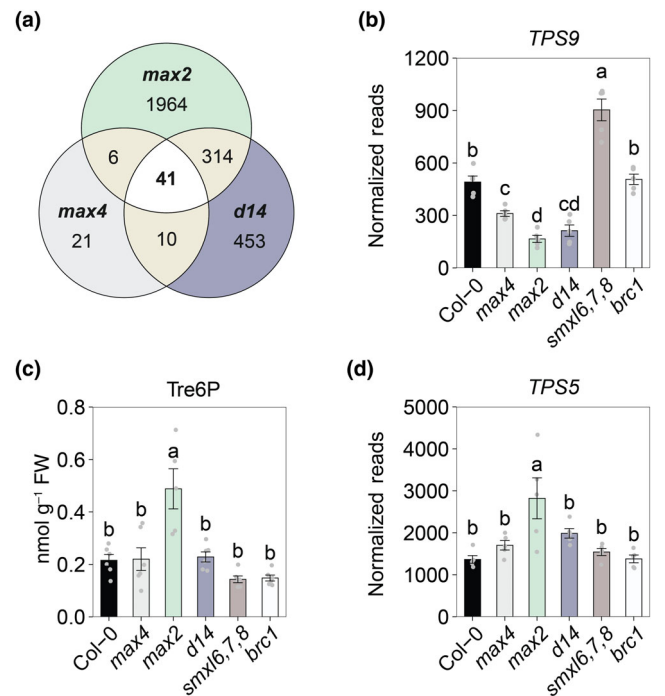


Fig. 2 Strigolactone mutants have alterations in trehalose 6-phosphate (Tre6P). (a) Overlap of differentially expressed genes (DEGs) in a strigolactone deficient (*max4*) and signalling (*max2* and *d14*) mutant of *Arabidopsis thaliana*. (b) Normalised RNA-seq reads (derived from DESeq2 analysis) of *TREHALOSE-6-PHOSPHATE SYNTHASE9* (*TPS9*) that is a DEG in all SL mutants. (c) Tre6P measurements of whole rosettes of *A. thaliana* strigolactone synthesis (*max4*), signalling (*max2*, *d14*) and downstream signalling (*smxl6,7,8* and *brc1*) mutant plants. (d) Normalised RNA-seq reads (derived from DESeq2 analysis) of *TREHALOSE-6-PHOSPHATE SYNTHASE5* (*TPS5*) which is a positive regulator of Tre6P signalling. Letters represent significant differences ($P < 0.05$) based on ANOVA with *post hoc* least significant difference (LSD) testing (mean \pm SE, $n = 5$ (RNA-seq), $n = 6$ (Tre6P)). *brc1*, *branched1*; *d14*, *dwarf14*; *max*, *more axillary growth*; *smxl6,7,8*, *suppressor of max2-like 6, 7 and 8*.

for sucrose efflux in phloem parenchyma, were significantly upregulated in *max2* mutants, with *SWEET11* showing a similar nonsignificant trend in *max4* and *d14* (Fig. S2b). Similarly, the Class II *TPS5* transcript was upregulated in *max2* mutants (Fig. 2d), with *TPS7* showing a similar behaviour (Fig. S3). In contrast to *TPS9*, *TPS5* and *TPS7* are downregulated upon carbon starvation (Ramon *et al.*, 2009). The upregulation of *TPS5* and *TPS7* in *max2* therefore aligns with the increased sugar and Tre6P levels and thus higher carbon availability in this mutant (Figs 2d, S2a). Increased levels of Tre6P, the downregulation of *TPS9*, the upregulation of *TPS5* and *TPS7*, and of *SWEET11* and *SWEET12* transcripts suggest that sugar signalling and allocation are altered in the *max2* mutant.

Trehalose 6-phosphate synthesis and signalling are altered in axillary buds of garden pea strigolactone mutants

To test these conclusions specifically in axillary buds, we used another model plant, garden pea, which has the advantage over Arabidopsis that axillary buds are larger and easier to access. This

can also provide evidence on potential conservation of regulatory relationships between SL and Tre6P. We monitored the expression of all pea *TPS* and *TPP* genes in node four axillary buds of the garden pea SL mutants *Psmax4* (*rms1*) and *Psmax2* (*rms4*). Homologues of the Arabidopsis TPS (Fig. S4a) and TPP (Fig. S4b) proteins in garden pea were identified by BLAST analysis on the pea proteome using the Arabidopsis homologues as query sequences followed by phylogenetic analyses using Bayesian and maximum likelihood approaches (Fig. S4; only clades with bootstrap values/posterior probabilities of > 65% are shown). These analyses revealed that there are three AtTPS1 homologues in garden pea termed PsTPS1.1-3 (Fig. S4a). Corroborating our results in Arabidopsis, the transcripts of all three TPS1 homologues were upregulated in axillary buds of *Psmax2* and *Psmax4* mutants when compared to WT plants (Fig. 3a). This upregulation was much stronger than the one observed in Arabidopsis further supporting that Tre6P likely increases specifically in axillary buds. We also found two homologues of the AtTPS8/AtTPS9/AtTPS10 clade which we termed PsTPS9 (Fig. S4a). Again corroborating our results in Arabidopsis rosettes, both TPS9 homologues were significantly downregulated in *Psmax2* axillary buds with *PsTPS9.2* also significantly downregulated in *Psmax4* (Fig. 3b). Lastly, to investigate whether SL mutants in pea also have high Tre6P levels, we measured Tre6P in axillary buds. Similar to results from Arabidopsis rosettes, *Psmax2* had significantly increased levels of Tre6P in axillary buds with *Psmax4* having the same trend (Fig. 3c). Due to the large variation in gene expression, there was no clear trend in the regulation of the *PsTPP* genes that were found to be expressed in axillary buds (Fig. S5a). There was also no change in the transcripts encoding the homologues of the class II TPS proteins AtTPS5, AtTPS6, or AtTPS7, while a homologue of AtTPS11 was downregulated in the *Psmax2* pea mutant (Fig. S5b).

Strigolactone mutants have alterations in Tre6P under certain conditions

The data in pea suggest that SL mutants have altered Tre6P levels and signalling in axillary buds. To test whether the increase in Tre6P is dependent on the light regime, Tre6P levels were also determined in *max4*, *max2* and *brc1* Arabidopsis mutants grown in long-day photoperiods with a decreased irradiance ($75 \mu\text{mol m}^{-2} \text{s}^{-1}$; Fig. S6a) and *max4*, *max2*, *d14* and *brc1* in short-day photoperiods with the same irradiance as before ($150 \mu\text{mol m}^{-2} \text{s}^{-1}$; Fig. S6b). These analyses showed that Tre6P was consistently higher in *max2* mutants (Fig. S6). In short-day photoperiods, Tre6P and sucrose were increased in *max2*, *max4* and *d14* mutants when harvested at the end of the day (Fig. S6b), showing that Tre6P is also increased in *max4* and *d14* mutants under certain conditions.

Increased levels of Tre6P in the vasculature increase branching in *brc1* mutants but not in strigolactone mutants

We demonstrated previously that an increase in Tre6P in the vasculature of *pGLDPA:otsA* construct lines induces early flowering

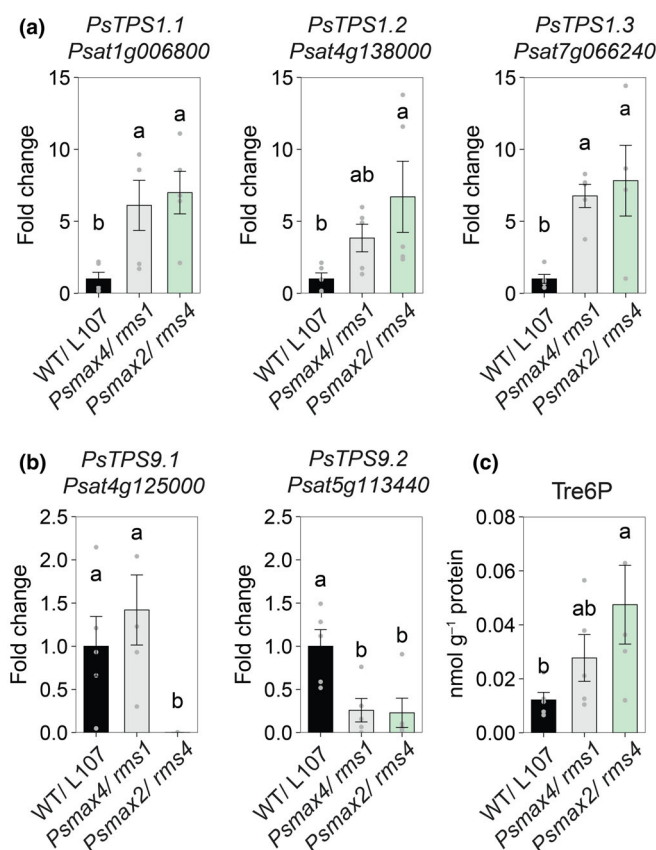


Fig. 3 Trehalose 6-phosphate (Tre6P) synthesis and signalling genes are altered in axillary buds of pea strigolactone mutants. (a) Quantitative reverse transcription polymerase chain reaction analysis of the genes encoding for the three homologues of TREHALOSE-6-PHOSPHATE SYNTHASE1 (TPS1) in garden pea (*Pisum sativum*) wild-type (WT) (L107) and *Psmax4* (*rms1*) and *Psmax2* (*rms4*) mutant plants. (b) Quantitative reverse transcription polymerase chain reaction analysis of the gene encoding for the two homologues of TREHALOSE-6-PHOSPHATE SYNTHASE9 (TPS9) in garden pea WT (L107) or *Psmax4* (*rms1*) and *Psmax2* (*rms4*) mutant plants. (c) Tre6P measurements of single axillary buds in garden pea WT (L107) and *Psmax4* (*rms1*) and *Psmax2* (*rms4*) mutant plants. Letters represent significant differences ($P < 0.05$) based on ANOVA with *post hoc* least significant difference (LSD) testing (mean \pm SE, $n = 5$). Node 4 buds of 11-d-old pea plants were analysed. *max*, more axillary growth; *rms*, ramosus.

and increases branching, likely via interaction with photoperiod signalling pathways and by altering sucrose allocation (Fichtner *et al.*, 2021a). This line expresses *OtsA/TPS* from *Escherichia coli* under the control of a vascular-tissue-specific promoter *GLYCINE-DECARBOXYLASE P-SUBUNIT A*, *GLDPA*, from *Flaveria trinervia* (hereafter referred to as the *High Tre6P* construct). To test whether the developmental responses altered by Tre6P are dependent on SL, we introgressed the *high Tre6P* construct into *max4*, *max2* and *brc1* to increase the levels of Tre6P in the vasculature (Fig. 4). We grew the resulting lines in two different irradiances ($150 \mu\text{mol m}^{-2} \text{s}^{-1}$, Fig. 4a; and $75 \mu\text{mol m}^{-2} \text{s}^{-1}$, Fig. 4b). The *High Tre6P* construct resulted in early flowering in WT plants, as expected (Fichtner *et al.*, 2021a), and also in all the mutant lines, showing that the

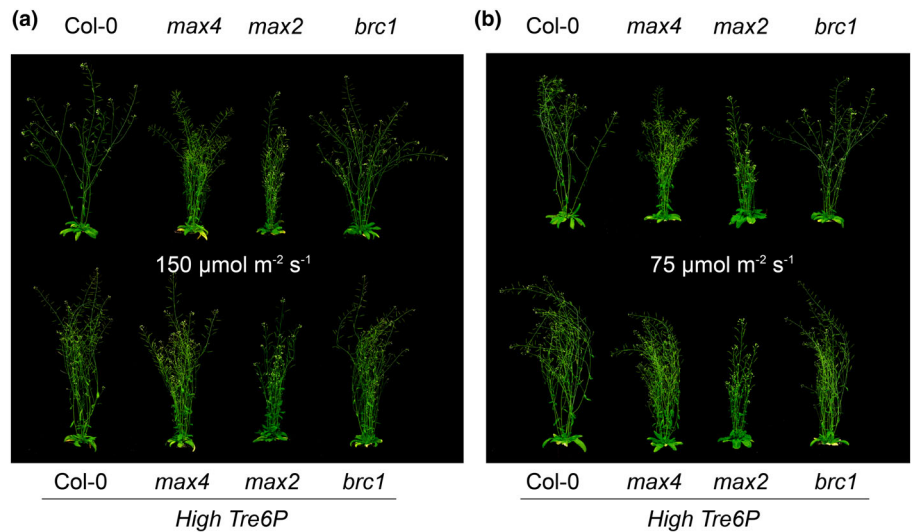
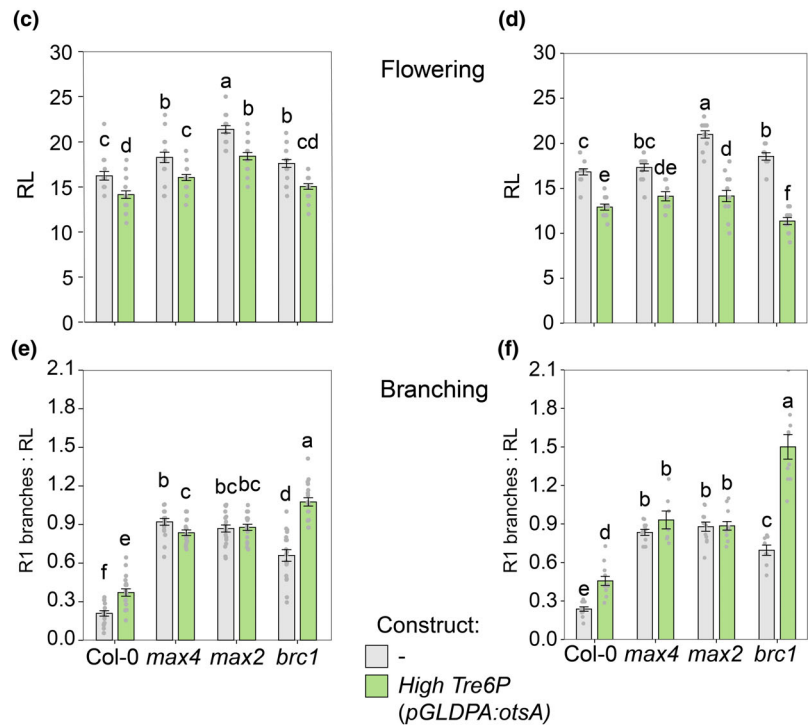


Fig. 4 Trehalose 6-phosphate (Tre6P) acts independently of *brc1* but dependent on strigolactone signalling in control of shoot branching. (a) Visual phenotype of *Arabidopsis thaliana* WT plants (Col-0), strigolactone synthesis (*max4*), signalling (*max2*) and *brc1* single mutant plants and plants with a construct conferring high Tre6P in the vasculature (*High Tre6P*, by expressing *otsA* using the vasculature-specific *pGLDPA* promoter, bottom panel) when grown in long days with an irradiance of 150 $\mu\text{mol photons m}^{-2} \text{s}^{-1}$. (b) The same genotypes grown under a lower irradiance of 75 $\mu\text{mol photons m}^{-2} \text{s}^{-1}$. (c) Flowering time as determined by the number of rosette leaves (RL) from plants in (a). (d) Flowering time as determined by RL from plants in (b). (e) Branching represented as the number of primary rosette branches (R1) normalised to RL (R1 : RL) from plants in (a). (f) Branching represented as R1 normalised to RL (R1 : RL) from plants in (b). Letters represent significant differences ($P < 0.05$) based on ANOVA with *post hoc* least significant difference (LSD) testing (mean \pm SE, $n = 17\text{--}20$). *max*, more axillary growth; *otsA*, Tre6P synthase from *Escherichia coli*; *pGLDPA*, GLYCINE-DECARBOXYLASE P-SUBUNIT A promoter from *Flaveria trinervia*.



induction of early flowering by high vascular Tre6P is independent of SL synthesis and signalling (Fig. 4c,d). This was also independent of the irradiance as Tre6P induced early flowering in both growth conditions.

To quantify shoot branching, we determined the number of primary rosette branches (R1), defined as the inflorescences (> 0.5 cm) that are initiated specifically from RL. Shoot branching was then expressed as the ratio R1 : RL since in SL mutants the number of R1 branches is strongly influenced by the number of RL (Fichtner *et al.*, 2022).

As previously observed, the introduction of the *High Tre6P* construct resulted in increased branching (R1 and R1 : RL) in the WT (Fichtner *et al.*, 2021a). The *High Tre6P* construct also resulted in increased branching in *brc1* mutant plants (Figs 4a,

b,e,f, S7). However, there was no increase in branching in *max4* or *max2* containing the *High Tre6P* construct (Figs 4a,b, e,f, S7) compared with the parental mutants, indicating that loss of SL synthesis and signalling prevents Tre6P promotion of branching. This lack of effect in SL mutants was not due to some limit on the maximum number of branches in *Arabidopsis* as the *brc1* mutant with the *high Tre6P* construct showed significantly more branching (10% increase in R1 : RL in 150 $\mu\text{mol m}^{-2} \text{s}^{-1}$, and 70% increase in R1 : RL in 75 $\mu\text{mol m}^{-2} \text{s}^{-1}$) than SL mutants (with or without the *High Tre6P* construct; Fig. 4e,f). Similar to SL deficient and perception mutants, the *High Tre6P* construct promoted flowering in *smxl6,7,8* mutants (Fig. S8a). The *High Tre6P* construct promoted shoot branching in *smxl6,7,8* mutants

(Fig. S8a), showing that the presence of SMXL proteins is not required for the branching response to high Tre6P.

In view of the dual role of MAX2 in shoot branching and karrikin signalling (Nelson *et al.*, 2011, 2012), we investigated *kai2*, a mutant deficient in karrikin perception. We tested for the dependence of Tre6P on the karrikin signalling pathway by analysing branching in *kai2* and in *kai2* plants containing the *High Tre6P* construct. We observed earlier flowering in *kai2* mutants expressing the *High Tre6P* construct, similar to other lines with this construct (Fig. S8b). The *kai2 high Tre6P* lines did not have significantly more R1 branches than WT Col-0, with or without the *High Tre6P* construct, or than the *kai2* parental mutant (Fig. S8b).

Lowering Tre6P can inhibit branching in *max2* mutant plants

One potential explanation for the inability of the *High Tre6P* construct to stimulate shoot branching in the SL synthesis or perception mutants is that Tre6P synthesis and/or signalling are already fully activated in these mutants. This could particularly be the case for *max2*, which has significantly higher levels of Tre6P than WT (Figs 2c, 3c, S6). To test this hypothesis, we generated a *max2* line with lower Tre6P levels by introducing a transgenic construct to express a *Caenorhabditis elegans* Tre6P phosphatase under the control of the vasculature-specific *GLDPA* promoter (Fichtner *et al.*, 2021a) (hereafter referred to as the *Low Tre6P* construct, Fig. 5a). The *Low Tre6P* construct delayed flowering in both the WT and the *max2* mutant (Fig. 5b). This result is consistent with an SL-independent role of Tre6P in flowering. Introduction of the *Low Tre6P* construct into WT and *max2* resulted in delayed branch emergence in both backgrounds (Figs 5c,d, S9) and a decreased final number of R1 : RL branches in *max2 low Tre6P* plants (Fig. 5c). To determine whether this delay in branch emergence coincided with decreased Tre6P levels, we determined Tre6P levels in *max2 low Tre6P* plants (Fig. 5e). This confirmed that *max2 low Tre6P* plants had significantly lower levels of Tre6P than *max2* mutants (Fig. 5e). The plants were also grown in lower light conditions ($75 \mu\text{mol m}^{-2} \text{s}^{-1}$, Fig. 5f). Flowering was delayed even further in *max2 low Tre6P* plants under these conditions. (Fig. 5g) and the delay in branch emergence was enhanced (Figs 5d,i, S9). At 14 d after bolting (dab), the *max2* plants with the *Low Tre6P* construct had only as many branches per leaf as WT plants, while the *max2* parental line had three times as many branches (Fig. 5h). Furthermore, at 14 dab *max2* with the *Low Tre6P* construct had the same number of branches as *max2* at 7 dab (Fig. 5h), showing that *Low Tre6P* caused a 7-d delay in branch emergence in *max2* under these conditions.

Another way of lowering sugar availability to the plants is growing them under carbon-limiting short-day conditions (8-h photoperiod). Under these conditions, *max2* containing the *Low Tre6P* construct also has a reduced final number of branches compared with *max2* (Fig. S10a), consistent with the hypothesis that lowering Tre6P in *max2* limits branching, especially under carbon-limiting conditions. Measurements of Tre6P in these

conditions confirmed that the *Low Tre6P* construct lowered Tre6P in the *max2* background (Fig. S10b).

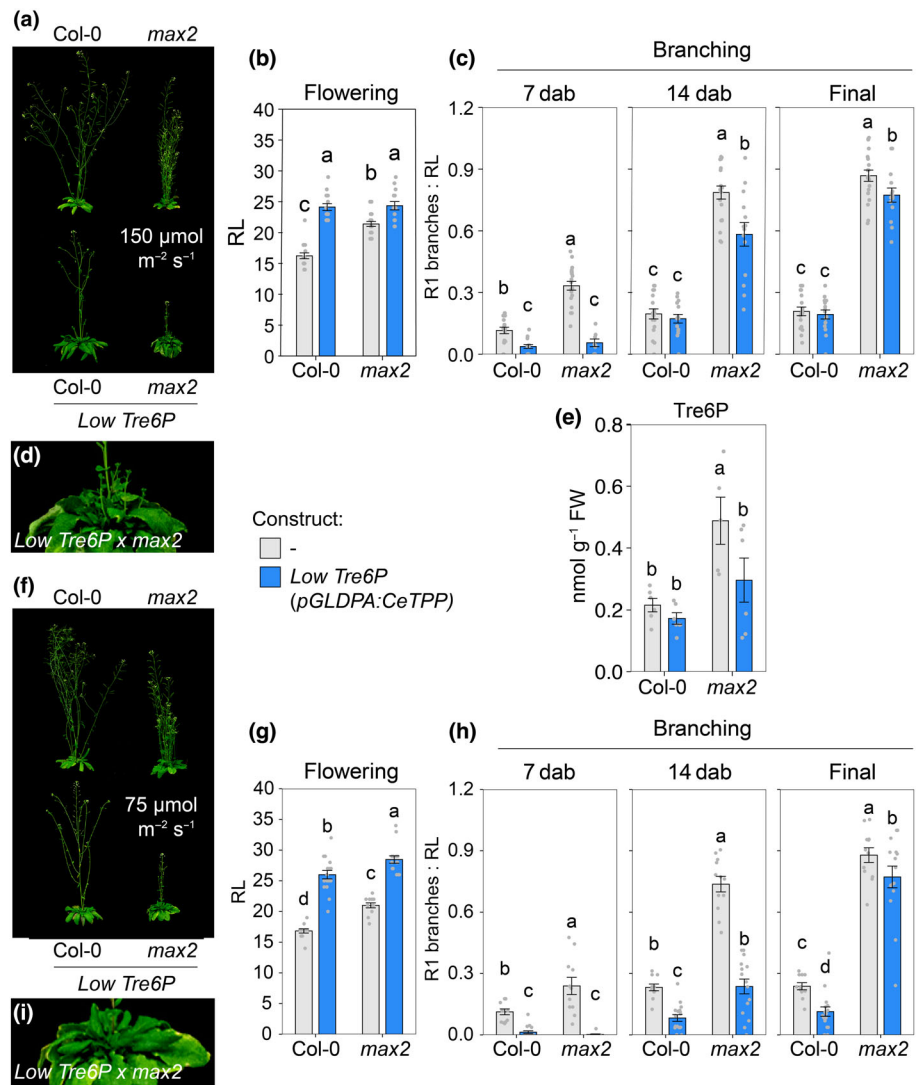
Lastly, we analysed the impact of the *High Tre6P* and *Low Tre6P* constructs on gene expression in WT and *max2* mutants by RNA-seq (Fig. 6a; Table S3). Hierarchical clustering of DEGs in all genotypes revealed that *max2* and *max2 high Tre6P* clustered together, suggesting a very similar transcript profile, possibly reflecting a predominant effect of the *max2* mutation. By contrast, *max2* with *Low Tre6P* and WT with *Low Tre6P* formed a separate cluster indicating that lowering Tre6P levels had a similar major effect in both of these genotypes (Fig. 6a). Cluster 2 stood out especially, as genes in this cluster showed high expression in branched mutants (*High Tre6P*, *max2*, *max2 high Tre6P*) and low expression in less branched mutants (*Low Tre6P*, *max2 low Tre6P*). GO term enrichment of this cluster did not reveal any consistently affected GO categories (Fig. S11); therefore, we used KEGG pathway enrichment (Fig. 6b). This analysis showed that metabolic pathways related to the 'TCA cycle' were highly enriched (16.7%, Fig. 6b). In addition, KEGG pathways related to amino acid synthesis were enriched. While gene expression cannot be used to simply infer metabolic flux, it is tempting to speculate that high Tre6P in the vasculature and in *max2* mutants might activate the metabolic flux into the TCA cycle, while low Tre6P in the vasculature has the opposite effect.

Discussion

The aim of this study was to understand how sugar signalling by Tre6P interacts with SL signalling to regulate shoot branching in Arabidopsis. We demonstrated that several genes related to Tre6P synthesis and signalling are differentially expressed in SL mutants in Arabidopsis and pea. We further observed that elevated Tre6P does not trigger additional shoot branching in mutants defective in SL biosynthesis (*max4*), perception (*d14*) and signalling (*max2*), and that *Low Tre6P* inhibits branching and strongly alters the transcript profile of *max2*. As Tre6P levels can be increased by SL signalling but excess Tre6P is not additive with SL deficiency, we suggest that the Tre6P pathway is one of the targets of SLs in regulating shoot branching. All genotypes tested showed early or delayed flowering in response to increased or decreased Tre6P levels, respectively, showing that the inability of Tre6P to promote branching in the SL mutants is not due to a general disruption of the response to Tre6P in these lines, but is specific to shoot branching.

Upon perception of SLs by D14, D14 forms an SCF complex with MAX2 that results in the polyubiquitination of SMXL6, 7 and 8 and de-repression of their targets (Wang *et al.*, 2022; Barbier *et al.*, 2023). One of these targets is the transcription factor BRC1, which represses shoot branching (Aguilar-Martínez *et al.*, 2007; van Es *et al.*, 2024). However, SLs only partially act via BRC1, as *brc1* mutants are less branched than SL mutants (Seale *et al.*, 2017; Fichtner *et al.*, 2022), suggesting a BRC1-independent role of SL signalling in the regulation of shoot branching. We showed here that the branch-promoting effect of Tre6P was independent of the SMXL6,7,8-BRC1 pathway. Indeed, our results showed that elevated Tre6P enhances shoot

Fig. 5 Lowering trehalose 6-phosphate (Tre6P) in *max2* can inhibit branching. (a) Visual phenotype of *Arabidopsis thaliana* plants with a construct conferring low Tre6P in the vasculature (*Low Tre6P*, by expressing *CeTTP* using the vasculature-specific *pGLDPA* promoter) and *max2* × *Low Tre6P* plants at 3 wk after bolting grown in long days with an irradiance of 150 $\mu\text{mol photons m}^{-2} \text{s}^{-1}$. (b) Flowering time as determined by the number of rosette leaves (RL). (c) Branching represented as the number of primary rosette branches (R1) normalised to RL ($R1 : RL$) at 7 or 14 d after bolting (dab), or at the end of the plant's life cycle (Final). (d) Magnified representation of (a) showing the R1 branches of *max2* × *Low Tre6P* plants. (e) Tre6P measurements of whole rosettes of plants grown in (a) harvested before bolting. (f) Visual phenotype of *Low Tre6P* and *max2* × *Low Tre6P* plants at 3 wk after bolting grown in long days with an irradiance of 75 $\mu\text{mol photons m}^{-2} \text{s}^{-1}$. (g) Flowering time as determined by RL. (h) Branching represented as R1 normalised to RL ($R1 : RL$) at 7 or 14 dab, or at the end of the plant's life cycle (Final). (i) Magnified representation of (f) showing the R1 branches of *max2* × *Low Tre6P* plants under lower light. Letters represent significant differences ($P < 0.05$) based on ANOVA with *post hoc* least significant difference (LSD) testing (mean \pm SE, $n = 11\text{--}17$). *CeTTP*, *Tre6P* phosphatase from *Caenorhabditis elegans*; *max*, *more axillary growth*; *pGLDPA*, *GLYCINE-DECARBOXYLASE P-SUBUNIT A promoter from Flaveria trinervia*.



branching in *smxl6,7,8* and *brc1* mutants. BRC1-independent regulation of shoot branching by SLs was previously reported by different studies, notably in pea and *Arabidopsis* (Braun *et al.*, 2012; Seale *et al.*, 2017). However, to our knowledge, no study so far has reported a SMXL6,7,8-independent effect of SLs on shoot branching. This could mean that there is another pathway that operates without the involvement of SMXL6,7,8 and that enables Tre6P to promote shoot branching. One such pathway might be mediated by the activation of *FLOWERING LOCUS T* and sucrose allocation via the SWEETs, as suggested previously (Fichtner *et al.*, 2021a) (Fig. 6c).

Our data showed that across different growth conditions, *max2* mutants consistently have elevated Tre6P levels, whereas the picture was more mixed in the other mutants. This suggests that MAX2 has an additional role in the regulation of Tre6P levels, beyond its role in integrating the SL signal. Besides SL perception, MAX2 mediates karrikin signalling through its interaction with KAI2, the karrikin-like compound receptor (Nelson *et al.*, 2011; Dun *et al.*, 2023). However, the *kai2* mutant has never been reported to have a shoot branching phenotype

(Bennett *et al.*, 2016b), ruling out the involvement of KAI2 in the regulation of this process. Surprisingly, *High Tre6P* did not significantly increase shoot branching in the *kai2* mutant. One interpretation of this result is that, in the absence of KAI2, more MAX2 protein is available for D14, reinforcing SL-derived signalling, and making it harder for Tre6P to alleviate the inhibitory effect of SL on shoot branching. In line with this, previous studies have shown that sucrose antagonises the effect of SL to promote axillary bud outgrowth (Bertheloot *et al.*, 2020; Patil *et al.*, 2022).

More recently, MAX2 was also reported to be involved in stomatal CO₂ signalling (Kalliola *et al.*, 2020) and to be inhibited by the TCA cycle intermediate citrate, at least *in vitro* (Tal *et al.*, 2022). This highlights the complexity of MAX2-dependent signalling and its central role in integrating hormonal and metabolic signals (Barbier *et al.*, 2023). During shoot branching, OsMAX2 has been reported to be the target of sugars to promote tillering in rice (Patil *et al.*, 2022). The higher accumulation of Tre6P in *max2* than in the other SL mutants further implicates a role for MAX2 in Tre6P-mediated carbon signalling during

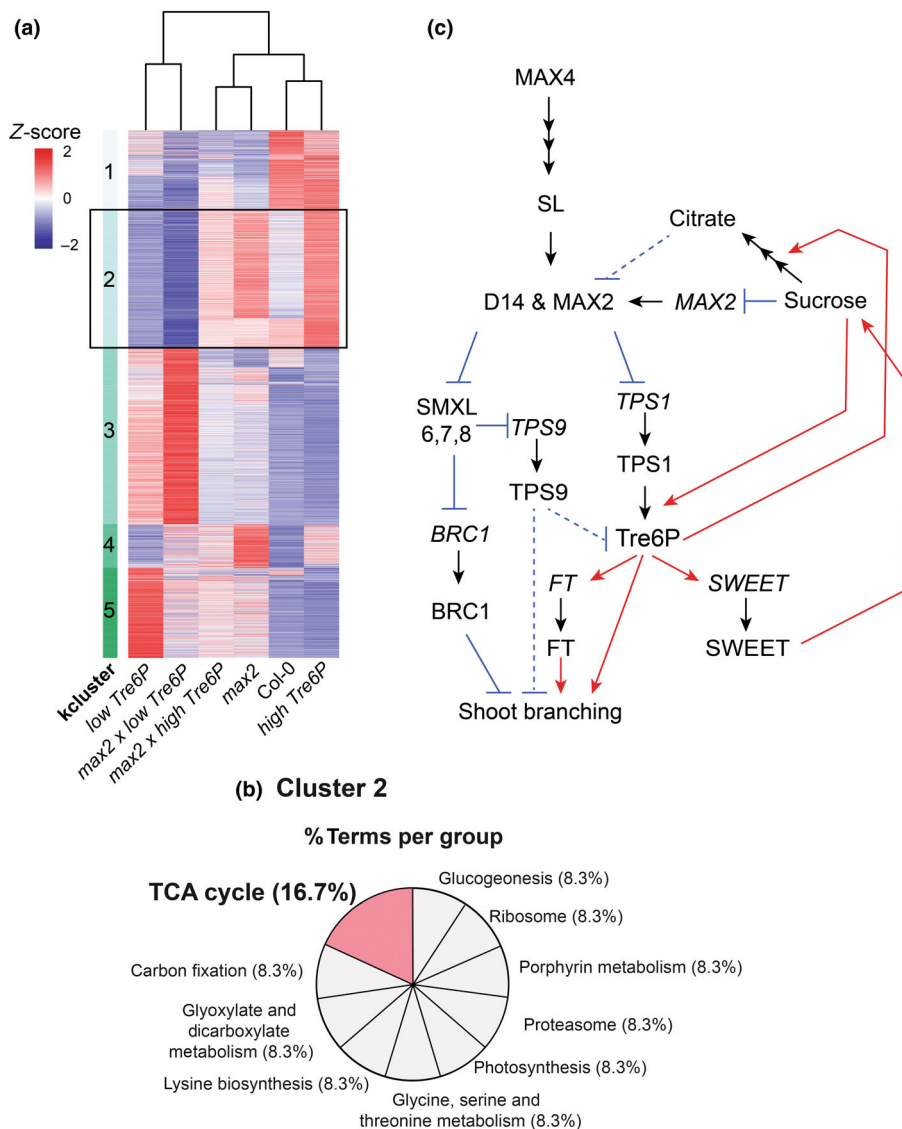


Fig. 6 Crosstalk between strigolactone, trehalose 6-phosphate (Tre6P) and sugar signalling pathways in the regulation of shoot branching. (a) K-means clustering of Z-scores of the means of normalised reads (from RNA-seq) of whole *Arabidopsis thaliana* rosettes of Col-0 plants, *max2*, *High Tre6P* (by expressing *otsA* using the vasculature-specific *pGLDPA* promoter) and *Low Tre6P* (by expressing *CeTPP* using the vasculature-specific *pGLDPA* promoter) mutants, as well as *max2* × *High Tre6P* and *max2* × *Low Tre6P* plants. Hierarchical clustering of the different genotypes is presented by a dendrogram. (b) KEGG pathway enrichment analysis of k-means Cluster 2. Percentages represent % of terms in group. (c) Schematic representation of the relationship between strigolactones, sucrose and Tre6P signalling. Tre6P is shown as being downstream of strigolactone signalling via a SUPPRESSOR OF MAX2-LIKE (SMXL)-dependent and independent pathway involving the inhibition of *TRE6P SYNTHASE1 (TPS1)* and *TPS9*. Tre6P acts in parallel to the known strigolactone signalling pathways involving *BRC1*. Tre6P also influences MAX2-dependent signalling by activating the flux into citrate which would lead to the inhibition of MAX2 on a protein level. This acts in parallel to the inhibition of MAX2 transcription by sucrose. Inhibition and activation are presented by blunt-ended blue or pointed red arrows, respectively. Currently, unknown interaction or interactions based on *in vitro* data are represented by dashed arrows. Black arrows represent processes. *BRC1*, *BRANCHED1*; *CeTPP*, *Tre6P phosphatase from Caenorhabditis elegans*; *max*, *more axillary growth*; *otsA*, *Tre6P synthase from Escherichia coli*; *pGLDPA*, *GLYCINE-DECARBOXYLASE P-SUBUNIT A promoter from Flaveria trinervia*; *SMXL*, *SUPPRESSOR OF MAX2-LIKE*.

shoot branching (Fig. 6c). Previous work has shown that a transient increase in Tre6P in *Arabidopsis* rosettes activates the anaplerotic flux of fixed carbon from photosynthesis into the TCA cycle by activating phosphoenolpyruvate carboxylase (PEPC). Isotope-labelling data suggested that the activation of PEPC is likely to be accompanied by the activation of the mitochondrial pyruvate dehydrogenase to increase flux around the TCA cycle (Figuroa *et al.*, 2016). A similar metabolic response was detected in axillary buds of garden pea after decapitation (Fichtner *et al.*, 2017). Tre6P increased rapidly in garden pea axillary buds after decapitation, and this increase coincided with a decrease in PEP and an increase in amino acids, suggesting higher flux of carbon into the TCA cycle and amino acid synthesis (Fichtner *et al.*, 2017). Citrate is readily transported between the mitochondria, cytosol and the vacuole (Abadie *et al.*, 2024). Therefore, the increased flux of carbon into the TCA cycle in response to higher Tre6P is likely to raise citrate levels in the cytosol, from where it could readily move into the nucleus to inhibit MAX2 activity (Barbier *et al.*, 2023). In agreement,

inhibition of flux into the TCA cycle has been demonstrated to inhibit lateral bud outgrowth in rose (Wang *et al.*, 2021). Our KEGG analysis in the SL mutants and Tre6P lines suggests that a similar mechanism is also activated by high Tre6P levels in the vasculature (Fig. 6b,c). This further supports the role of Tre6P in modulating citrate levels and metabolism and opens the possibility for a feedback loop between MAX2 and Tre6P signalling pathways (Fig. 6c). More work is needed to further test this hypothesis.

Loss of *BRC1* combined with *High Tre6P* results in a shoot branching phenotype similar to that of SL mutants, as *brc1 high Tre6P* mutants showed a strong increase in branching when compared to *brc1* single mutants. This is consistent with the hypothesis that Tre6P signalling is downstream of SL signalling but acts in parallel to the SMXL6,7,8-dependent inhibition of *BRC1* (Fig. 6c). Loss of *BRC1* together with high Tre6P levels would therefore mimic a complete loss of SL signalling. It is worth noting that *brc1 high Tre6P* mutants do not show any other of the typical phenotypes of SL mutants, like dwarfism or a different

leaf shape, suggesting that the function of *high Tre6P* in the *brc1* mutant specifically modulates shoot branching.

The increased expression of *TPS1* in *max4*, *max2* and *d14* mutants in Arabidopsis is accompanied by increased Tre6P levels in the mutants, under at least some growth conditions (Figs 2, 3, 5e). In a recent review, Barbier *et al.* describe SLs as playing a central role in the control of plant shoot architecture by the plant's nutritional status and environment (Barbier *et al.*, 2023). Analyses of individual axillary buds from orthologous garden pea SL mutants showed that expression of *PstTPS1* genes was increased in the buds themselves (Fig. 3a), compared with WT, as were the levels of Tre6P (Fig. 3c). These results suggest that MAX2-dependent SL signalling inhibits Tre6P synthesis in axillary buds by inhibiting expression of *TPS1* and its orthologs in pea.

TPS9 expression was downregulated in *max4*, *max2* and *d14* mutants and the expression of genes encoding TPS9 homologues in pea was also reduced in axillary buds, suggesting that *TPS9* is a target of SL signalling. This further supports the idea of the Tre6P pathway being downstream of SLs in the regulation of bud outgrowth. Similarly, transcriptional profiling of dormant and vernalisation-released buds of the perennial model species *Arabis alpina* showed decreased expression of *AaTPS9* (Vayssières *et al.*, 2020). In addition, *TPS9* expression was upregulated in the *smxl6,7,8* mutants of Arabidopsis, indicating that SLs act through these SMXLs to regulate *TPS9* expression. In agreement with this hypothesis, SMXL6 was found to bind to the 5'-UTR of the *TPS9* gene (Wang *et al.*, 2020). Despite Tre6P acting independently of SMXL6,7,8, Tre6P and SL signalling are intricately interconnected (Fig. 6c). This is also in line with observations indicating that the BRC1/TB1 transcription factor targets genes involved in Tre6P homeostasis (Dong *et al.*, 2019). More work is needed to unravel the specific molecular mechanisms underpinning these interactions.

In conclusion, our study shows that SLs act partly via Tre6P to control shoot branching in a BRC1-independent manner (Fig. 6c). Since SL perception is controlled by sugar availability and potentially by other metabolites from primary metabolism, such as citrate, our study highlights the intricate connection between SL and sugar signalling pathways during the control of shoot branching. It is tempting to speculate that this link between primary metabolism and hormonal regulation of shoot branching evolved to guarantee the high responsiveness of shoot branching to the environment (de Jong *et al.*, 2014, 2019; Fichtner *et al.*, 2022; Kelly *et al.*, 2023).

Acknowledgements

We thank the CEPLAS metabolomics team as well as Lindsay Shaw, Sophie Jones, Caitlin Dudley, Alicia Hellens and Hannah Driberg for technical assistance and help with plant work. We thank Mark Stitt for helpful discussions and comments on the manuscript. This work was supported by the Australian Research Council (FFB, FF, CAB, JLH and SMS, Centre of Excellence CE200100015, and FFB, FF, CAB, the Georgina Sweet Laureate Fellowship FL180100139), the Max Planck Society (RF and

JEL) and the German Research Foundation/Deutsche Forschungsgemeinschaft (research grant awarded to FF, project no.: 515360083, grant no.: FI 2664/2-1, and CEPLAS under Germany's Excellence Strategy, FF, PW, project no.: 390686111, grant no.: EXC 2048/1).

Competing interests

None declared.

Author contributions

FF and CAB conceived the project. FF designed and performed all experiments with help from FFB except for quantitative reverse transcription polymerase chain reaction analyses. JLH performed quantitative reverse transcription polymerase chain reaction. JLH performed the RNA-seq analyses with initial data processing done by FF. RF, JEL and PW performed Tre6P measurements. AM assisted in synthesising an internal Tre6P standard for Tre6P measurements by PW and FF. FF wrote the manuscript with support from CAB, JEL, SMS and FFB. All authors commented on the manuscript and approved the final version. JLH and FFB contributed equally to this study.

ORCID

Francois F. Barbier  <https://orcid.org/0000-0002-1177-1930>

Christine A. Beveridge  <https://orcid.org/0000-0003-0878-3110>

Regina Feil  <https://orcid.org/0000-0002-9936-1337>

Franziska Fichtner  <https://orcid.org/0000-0002-4508-5437>

Jasmine L. Humphreys  <https://orcid.org/0000-0003-3546-887X>

John E. Lunn  <https://orcid.org/0000-0001-8533-3004>

Anna Moseler  <https://orcid.org/0000-0003-4641-8093>

Steven M. Smith  <https://orcid.org/0000-0001-5661-9994>

Philipp Westhoff  <https://orcid.org/0000-0002-3494-9420>

Data availability

All RNA-seq data described in this study have been deposited in the NCBI Short Read Archive (SRA) database under <http://www.ncbi.nlm.nih.gov/bioproject/934161> (Submission ID: SUB12863317, BioProject ID: PRJNA934161).

References

- Abadie C, Lalande J, Dourmap C, Limami AM, Tcherkez G. 2024. Leaf day respiration involves multiple carbon sources and depends on previous dark metabolism. *Plant, Cell & Environment* 47: 2146–2162.
- Afgan E, Baker D, van den Beek M, Blankenberg D, Bouvier D, Cech M, Chilton J, Clements D, Coraor N, Eberhard C *et al.* 2016. The Galaxy platform for accessible, reproducible and collaborative biomedical analyses: 2016 update. *Nucleic Acids Research* 44: W3–W10.
- Aguilar-Martínez JA, Poza-Carrión C, Cubas P. 2007. Arabidopsis BRANCHED1 acts as an integrator of branching signals within axillary buds. *Plant Cell* 19: 458–472.

- Andrews S. 2010. *FASTQC: a quality control tool for high throughput sequence data*. Cambridge, UK: Babraham Bioinformatics, Babraham Institute.
- Arite T, Umehara M, Ishikawa S, Hanada A, Maekawa M, Yamaguchi S, Kyojuka J. 2009. A strigolactone-insensitive mutant of rice, shows an accelerated outgrowth of tillers. *Plant and Cell Physiology* 50: 1416–1424.
- Barbier FF, Cao D, Fichtner F, Weiste C, Perez-Garcia MD, Caradeuc M, Le Gourrierec J, Sakr S, Beveridge CA. 2021. HEXOKINASE1 signalling promotes shoot branching and interacts with cytokinin and strigolactone pathways. *New Phytologist* 231: 1088–1104.
- Barbier FF, Chabikwa TG, Ahsan MU, Cook SE, Powell R, Tanurdzic M, Beveridge CA. 2019a. A phenol/chloroform-free method to extract nucleic acids from recalcitrant, woody tropical species for gene expression and sequencing. *Plant Methods* 15: 1–13.
- Barbier FF, Dun EA, Kerr SC, Chabikwa TG, Beveridge CA. 2019b. An update on the signals controlling shoot branching. *Trends in Plant Science* 24: 220–236.
- Barbier FF, Fichtner F, Beveridge C. 2023. The strigolactone pathway plays a crucial role in integrating metabolic and nutritional signals in plants. *Nature Reviews* 9: 1191–1200.
- Barbier FF, Péron T, Lecerf M, Perez-Garcia MD, Barrière Q, Rolcic J, Boutet-Mercey S, Citerne S, Lemoine R, Porcheron B *et al.* 2015. Sucrose is an early modulator of the key hormonal mechanisms controlling bud outgrowth in. *Journal of Experimental Botany* 66: 2569–2582.
- Bennett T, Hines G, van Rongen M, Waldie T, Sawchuk MG, Scarpella E, Ljung K, Leyser O. 2016a. Connective auxin transport in the shoot facilitates communication between shoot apices. *PLoS Biology* 14: e1002446.
- Bennett T, Liang Y, Seale M, Ward S, Müller D, Leyser O. 2016b. Strigolactone regulates shoot development through a core signalling pathway. *Biology Open* 5: 1806–1820.
- Bennett T, Sieberer T, Willett B, Booker J, Luschnig C, Leyser O. 2006. The Arabidopsis MAX pathway controls shoot branching by regulating auxin transport. *Current Biology* 16: 553–563.
- Bertheloot J, Barbier F, Boudon F, Perez-Garcia MD, Peron T, Citerne S, Dun E, Beveridge C, Godin C, Sakr S. 2020. Sugar availability suppresses the auxin-induced strigolactone pathway to promote bud outgrowth. *New Phytologist* 225: 866–879.
- Beveridge CA, Murfet IC, Kerhoas L, Sotta B, Miginiac E, Rameau C. 1997a. The shoot controls zeatin riboside export from pea roots. Evidence from the branching mutant *rms4*. *The Plant Journal* 11: 339–345.
- Beveridge CA, Symons GM, Murfet IC, Ross JJ, Rameau C. 1997b. The *rms1* mutant of pea has elevated indole-3-acetic acid levels and reduced root-sap zeatin riboside content but increased branching controlled by graft-transmissible signal(s). *Plant Physiology* 115: 1251–1258.
- Bindea G, Mlecnik B, Hackl H, Charoentong P, Tosolini M, Kirilovsky A, Fridman WH, Pages F, Trajanoski Z, Galon J. 2009. CLUEGO: a Cytoscape plug-in to decipher functionally grouped gene ontology and pathway annotation networks. *Bioinformatics* 25: 1091–1093.
- Booker J, Sieberer T, Wright W, Williamson L, Willett B, Stirnberg P, Turnbull C, Srinivasan M, Goddard P, Leyser O. 2005. MAX1 encodes a cytochrome P450 family member that acts downstream of MAX3/4 to produce a carotenoid-derived branch-inhibiting hormone. *Developmental Cell* 8: 443–449.
- Braun N, de Saint GA, Pillot JP, Boutet-Mercey S, Dalmais M, Antoniadis I, Li X, Maia-Grondard A, Le Signor C, Bouteiller N *et al.* 2012. The pea TCP transcription factor PsBRC1 acts downstream of Strigolactones to control shoot branching. *Plant Physiology* 158: 225–238.
- Brewer PB, Koltai H, Beveridge CA. 2013. Diverse roles of strigolactones in plant development. *Molecular Plant* 6: 18–28.
- Cao D, Chabikwa T, Barbier F, Dun EA, Fichtner F, Dong L, Kerr SC, Beveridge CA. 2023. Auxin-independent effects of apical dominance induce changes in phytohormones correlated with bud outgrowth. *Plant Physiology* 192: 1420–1434.
- Cheng CY, Krishnakumar V, Chan AP, Thibaud-Nissen F, Schobel S, Town CD. 2017. Araport11: a complete reannotation of the *Arabidopsis thaliana* reference genome. *The Plant Journal* 89: 789–804.
- Chevalier F, Nieminen K, Sanchez-Ferrero JC, Rodriguez ML, Chagoyen M, Hardtke CS, Cubas P. 2014. Strigolactone promotes degradation of DWARF14, an alpha/beta hydrolase essential for strigolactone signaling in Arabidopsis. *Plant Cell* 26: 1134–1150.
- Crawford S, Shinohara N, Sieberer T, Williamson L, George G, Hepworth J, Müller D, Domagalska MA, Leyser O. 2010. Strigolactones enhance competition between shoot branches by dampening auxin transport. *Development* 137: 2905–2913.
- Domagalska MA, Leyser O. 2011. Signal integration in the control of shoot branching. *Nature Reviews. Molecular Cell Biology* 12: 211–221.
- Dong Z, Xiao Y, Govindarajulu R, Feil R, Siddoway ML, Nielsen T, Lunn JE, Hawkins J, Whipple C, Chuck G. 2019. The regulatory landscape of a core maize domestication module controlling bud dormancy and growth repression. *Nature Communications* 10: 3810.
- Dun EA, Brewer PB, Gillam EM, Beveridge CA. 2023. Strigolactones and shoot branching: what is the real hormone and how does it work? *Plant and Cell Physiology* 64: 967–983.
- van Es SW, Muñoz-Gasca A, Romero-Campero FJ, González-Grandío E, de Los RP, Tarancón C, van Dijk AD, van Esse W, Pascual-García A, Angenent GC. 2024. A gene regulatory network critical for axillary bud dormancy directly controlled by Arabidopsis BRANCHED1. *New Phytologist* 241: 1193–1209.
- Fichtner F, Barbier FF, Annunziata MG, Feil R, Olas JJ, Mueller-Roeber B, Stitt M, Beveridge CA, Lunn JE. 2021a. Regulation of shoot branching in Arabidopsis by trehalose 6-phosphate. *New Phytologist* 229: 2135–2151.
- Fichtner F, Barbier FF, Feil R, Watanabe M, Annunziata MG, Chabikwa TG, Höfgen R, Stitt M, Beveridge CA, Lunn JE. 2017. Trehalose 6-phosphate is involved in triggering axillary bud outgrowth in garden pea (*Pisum sativum* L.). *The Plant Journal* 92: 611–623.
- Fichtner F, Barbier FF, Kerr SC, Dudley C, Cubas P, Turnbull C, Brewer PB, Beveridge CA. 2022. Plasticity of bud outgrowth varies at cauline and rosette nodes in *Arabidopsis thaliana*. *Plant Physiology* 188: 1586–1603.
- Fichtner F, Dissanayake IM, Lacombe B, Barbier F. 2021b. Sugar and nitrate sensing: a multi-billion-year story. *Trends in Plant Science* 26: 352–374.
- Fichtner F, Lunn JE. 2021. The role of Trehalose 6-Phosphate (Tre6P) in plant metabolism and development. *Annual Review of Plant Biology* 72: 737–760.
- Fichtner F, Olas JJ, Feil R, Watanabe M, Krause U, Hoefgen R, Stitt M, Lunn JE. 2020. Functional features of TREHALOSE-6-PHOSPHATE SYNTHASE1, an essential enzyme in Arabidopsis. *Plant Cell* 32: 1949–1972.
- Figuerola CM, Feil R, Ishihara H, Watanabe M, Kolling K, Krause U, Hohne M, Encke B, Plaxton WC, Zeeman SC *et al.* 2016. Trehalose 6-phosphate coordinates organic and amino acid metabolism with carbon availability. *The Plant Journal* 85: 410–423.
- Göbel M, Fichtner F. 2023. Functions of sucrose and trehalose 6-phosphate in controlling plant development. *Journal of Plant Physiology* 15: 154140.
- Guindon S, Dufayard J-F, Lefort V, Anisimova M, Hordijk W, Gascuel O. 2010. New algorithms and methods to estimate maximum-likelihood phylogenies: assessing the performance of PHYML 3.0. *Systematic Biology* 59: 307–321.
- Ha CV, Leyva-Gonzalez MA, Osakabe Y, Tran UT, Nishiyama R, Watanabe Y, Tanaka M, Seki M, Yamaguchi S, Dong NV *et al.* 2014. Positive regulatory role of strigolactone in plant responses to drought and salt stress. *Proceedings of the National Academy of Sciences, USA* 111: 851–856.
- Hamiaux C, Drummond RSM, Janssen BJ, Ledger SE, Cooney JM, Newcomb RD, Snowden KC. 2012. DAD2 is an α/β hydrolase likely to be involved in the perception of the plant branching hormone, strigolactone. *Current Biology* 22: 2032–2036.
- Hellens AM, Chabikwa TG, Fichtner F, Brewer PB, Beveridge CA. 2023. Identification of new potential downstream transcriptional targets of the strigolactone pathway including glucosinolate biosynthesis. *Plant Direct* 7: e486.
- Huelsenbeck JP, Ronquist F. 2001. MRBAYES: bayesian inference of phylogenetic trees. *Bioinformatics* 17: 754–755.
- Jiang L, Liu X, Xiong GS, Liu HH, Chen FL, Wang L, Meng XB, Liu GF, Yu H, Yuan YD *et al.* 2013. DWARF 53 acts as a repressor of strigolactone signalling in rice. *Nature* 504: 401.
- de Jong M, George G, Ongaro V, Williamson L, Willetts B, Ljung K, McCulloch H, Leyser O. 2014. Auxin and strigolactone signaling are required for modulation of Arabidopsis shoot branching by nitrogen supply. *Plant Physiology* 166: 384–395.

- de Jong M, Tavares H, Pasam RK, Butler R, Ward S, George G, Melnyk CW, Challis R, Kover PX, Leyser O. 2019. Natural variation in Arabidopsis shoot branching plasticity in response to nitrate supply affects fitness. *PLoS Genetics* 15: e1008366.
- Kalliola M, Jakobson L, Davidsson P, Pennanen V, Waszczak C, Yarmolinsky D, Zamora O, Palva ET, Kariola T, Kollist H *et al.* 2020. Differential role of MAX2 and strigolactones in pathogen, ozone, and stomatal responses. *Plant Direct* 4: e00206.
- Kelly JH, Tucker MR, Brewer PB. 2023. The strigolactone pathway is a target for modifying crop shoot architecture and yield. *Biology* 12: 95.
- Kreplak J, Madoui M-A, Cápál P, Novák P, Labadie K, Aubert G, Bayer PE, Gali KK, Syme RA, Main D. 2019. A reference genome for pea provides insight into legume genome evolution. *Nature Genetics* 51: 1411–1422.
- Lantzouni O, Klermund C, Schwechheimer C. 2017. Largely additive effects of gibberellin and strigolactone on gene expression in *Arabidopsis thaliana* seedlings. *The Plant Journal* 92: 924–938.
- Li W, Nguyen KH, Chu HD, Watanabe Y, Osakabe Y, Sato M, Toyooka K, Seo M, Tian L, Tian C *et al.* 2020. Comparative functional analyses of DWARF14 and KARRIKIN INSENSITIVE 2 in drought adaptation of *Arabidopsis thaliana*. *The Plant Journal* 103: 111–127.
- Love M, Anders S, Huber W. 2014. Differential analysis of count data—the DESeq2 package. *Genome Biology* 15: 10–1186.
- Lunn JE. 2007. Gene families and evolution of trehalose metabolism in plants. *Functional Plant Biology* 34: 550–563.
- Lunn JE, Feil R, Hendriks JH, Gibon Y, Morcuende R, Osuna D, Scheible WR, Carillo P, Hajirezaei MR, Stitt M. 2006. Sugar-induced increases in trehalose 6-phosphate are correlated with redox activation of ADPglucose pyrophosphorylase and higher rates of starch synthesis in *Arabidopsis thaliana*. *The Biochemical Journal* 397: 139–148.
- Luo Z, Janssen BJ, Snowden KC. 2021. The molecular and genetic regulation of shoot branching. *Plant Physiology* 187: 1033–1044.
- Mason MG, Ross JJ, Babst BA, Wienclaw BN, Beveridge CA. 2014. Sugar demand, not auxin, is the initial regulator of apical dominance. *Proceedings of the National Academy of Sciences, USA* 111: 6092–6097.
- Morris SE, Cox MC, Ross JJ, Krisantini S, Beveridge CA. 2005. Auxin dynamics after decapitation are not correlated with the initial growth of axillary buds. *Plant Physiology* 138: 1665–1672.
- Nahas Z, Ticchiarelli F, van Rongen M, Dillon J, Leyser O. 2024. The activation of Arabidopsis axillary buds involves a switch from slow to rapid committed outgrowth regulated by auxin and strigolactone. *New Phytologist* 242: 1084–1097.
- Nelson DC, Flematti GR, Ghisalberti EL, Dixon KW, Smith SM. 2012. Regulation of seed germination and seedling growth by chemical signals from burning vegetation. *Annual Review of Plant Biology* 63: 107–130.
- Nelson DC, Scaffidi A, Dun EA, Waters MT, Flematti GR, Dixon KW, Beveridge CA, Ghisalberti EL, Smith SM. 2011. F-box protein MAX2 has dual roles in karrikin and strigolactone signaling in. *Proceedings of the National Academy of Sciences, USA* 108: 8897–8902.
- Patil SB, Barbier FF, Zhao J, Zafar SA, Uzair M, Sun Y, Fang J, Perez-Garcia MD, Bertheloot J, Sakr S *et al.* 2022. Sucrose promotes D53 accumulation and tillering in rice. *New Phytologist* 234: 122–136.
- Patro R, Duggal G, Love MI, Irizarry RA, Kingsford C. 2017. Salmon provides fast and bias-aware quantification of transcript expression. *Nature Methods* 14: 417–419.
- Prusinkiewicz P, Crawford S, Smith RS, Ljung K, Bennett T, Ongaro V, Leyser O. 2009. Control of bud activation by an auxin transport switch. *Proceedings of the National Academy of Sciences, USA* 106: 17431–17436.
- Ramon M, De Smet I, Vandesteene L, Naudts M, Leyman B, Van Dijck P, Rolland F, Beeckman T, Thevelein JM. 2009. Extensive expression regulation and lack of heterologous enzymatic activity of the Class II trehalose metabolism proteins from *Arabidopsis thaliana*. *Plant, Cell & Environment* 32: 1015–1032.
- Salam BB, Barbier F, Danielli R, Teper-Bamnolker P, Ziv C, Spichal L, Aruchamy K, Shnaider Y, Leibman D, Shaya F. 2021. Sucrose promotes stem branching through cytokinin. *Plant Physiology* 185: 1708–1721.
- Seale M, Bennett T, Leyser O. 2017. BRC1 expression regulates bud activation potential but is not necessary or sufficient for bud growth inhibition in Arabidopsis. *Development* 144: 1661–1673.
- Shinohara N, Taylor C, Leyser O. 2013. Strigolactone can promote or inhibit shoot branching by triggering rapid depletion of the auxin efflux protein PIN1 from the plasma membrane. *PLoS Biology* 11: e1001474.
- Sorefan K, Booker J, Haurigné K, Goussot M, Bainbridge K, Foo E, Chatfield S, Ward S, Beveridge C, Rameau C. 2003. MAX4 and RMS1 are orthologous dioxygenase-like genes that regulate shoot branching in Arabidopsis and pea. *Genes & Development* 17: 1469–1474.
- Soundappan I, Bennett T, Morffy N, Liang Y, Stanga JP, Abbas A, Leyser O, Nelson DC. 2015. SMAX1-LIKE/D53 family members enable distinct MAX2-dependent responses to strigolactones and karrikins in Arabidopsis. *Plant Cell* 27: 3143–3159.
- Stirnberg P, Furner IJ, Leyser HMO. 2007. MAX2 participates in an SCF complex which acts locally at the node to suppress shoot branching. *The Plant Journal* 50: 80–94.
- Stirnberg P, van De Sande K, Leyser HM. 2002. MAX1 and MAX2 control shoot lateral branching in Arabidopsis. *Development* 129: 1131–1141.
- Stitt M, Lilley RM, Gerhardt R, Heldt HW. 1989. [32] Metabolite levels in specific cells and subcellular compartments of plant leaves. *Methods in Enzymology* 20: 518–552.
- Tal L, Palayam M, Ron M, Young A, Britt A, Shabek N. 2022. A conformational switch in the SCF-D3/MAX2 ubiquitin ligase facilitates strigolactone signalling. *Nature Plants* 8: 561–573.
- Van Leene J, Eeckhout D, Gadeyne A, Matthijs C, Han C, De Winne N, Persiau G, Van De Slijke E, Peryns F, Mertens T *et al.* 2022. Mapping of the plant SnRK1 kinase signalling network reveals a key regulatory role for the class II T6P synthase-like proteins. *Nature Plants* 8: 1245–1261.
- Vandesteene L, Ramon M, Le Roy K, Van Dijck P, Rolland F. 2010. A single active trehalose-6-P synthase (TPS) and a family of putative regulatory TPS-like proteins in Arabidopsis. *Molecular Plant* 3: 406–419.
- Vayssières A, Mishra P, Roggen A, Neumann U, Ljung K, Albani MC. 2020. Vernalization shapes shoot architecture and ensures the maintenance of dormant buds in the perennial *Arabis alpina*. *New Phytologist* 227: 99–115.
- Wang L, Wang B, Jiang L, Liu X, Li X, Lu Z, Meng X, Wang Y, Smith SM, Li J. 2015. Strigolactone signaling in Arabidopsis regulates shoot development by targeting D53-Like SMXL repressor proteins for ubiquitination and degradation. *Plant Cell* 27: 3128–3142.
- Wang L, Wang B, Yu H, Guo H, Lin T, Kou L, Wang A, Shao N, Ma H, Xiong G *et al.* 2020. Transcriptional regulation of strigolactone signalling in Arabidopsis. *Nature* 583: 277–281.
- Wang M, Pérez-García MD, Davière JM, Barbier F, Ogé L, Gentilhomme J, Voisine L, Péron T, Launay-Avon A, Clément G *et al.* 2021. Outgrowth of the axillary bud in rose is controlled by sugar metabolism and signalling. *Journal of Experimental Botany* 72: 3044–3060.
- Wang Q, Smith SM, Huang J. 2022. Origins of strigolactone and karrikin signaling in plants. *Trends in Plant Science* 27: 450–459.
- Waters MT, Scaffidi A, Moulin SL, Sun YK, Flematti GR, Smith SM. 2015. A Selaginella moellendorffii ortholog of KARRIKIN INSENSITIVE2 functions in Arabidopsis development but cannot mediate responses to Karrikins or Strigolactones. *Plant Cell* 27: 1925–1944.
- Yadav UP, Ivakov A, Feil R, Duan GY, Walther D, Giavalisco P, Piques M, Carillo P, Hubberten HM, Stitt M *et al.* 2014. The sucrose-trehalose 6-phosphate (Tre6P) nexus: specificity and mechanisms of sucrose signalling by Tre6P. *Journal of Experimental Botany* 65: 1051–1068.
- Zang B, Li H, Li W, Deng XW, Wang X. 2011. Analysis of trehalose-6-phosphate synthase (TPS) gene family suggests the formation of TPS complexes in rice. *Plant Molecular Biology* 76: 507–522.

Supporting Information

Additional Supporting Information may be found online in the Supporting Information section at the end of the article.

Fig. S1 Expression of Arabidopsis *TREHALOSE-6-PHOSPHATE PHOSPHATASE* genes in strigolactone mutants.

Fig. S2 Sucrose and trehalose 6-phosphate : sucrose ratios in different strigolactone mutants.

Fig. S3 Expression of Arabidopsis *TREHALOSE-6-PHOSPHATE SYNTHASE* genes in strigolactone mutants.

Fig. S4 Identification of the *TREHALOSE-6-PHOSPHATE SYNTHASE* and *TREHALOSE-6-PHOSPHATE PHOSPHATASE* protein family in garden pea (*Pisum sativum*).

Fig. S5 Expression of trehalose 6-phosphate synthesis and signalling genes in axillary buds of pea strigolactone mutants.

Fig. S6 Trehalose 6-phosphate levels, sucrose levels and Tre6P : sucrose ratios in different strigolactone mutants.

Fig. S7 Trehalose 6-phosphate induces branching in *brc1* but not *max4* or *max2* mutants.

Fig. S8 Trehalose 6-phosphate induces branching in *smxl6,7,8* but not *kai2* mutants.

Fig. S9 Lowering trehalose 6-phosphate in *max2* can inhibit branching in long days.

Fig. S10 Lowering trehalose 6-phosphate inhibits branching in *max2* mutants in short-day conditions.

Fig. S11 GO term enrichment analysis of a k-means cluster that contained genes that showed high expression in branched mutants did not reveal any consistently affected GO categories.

Table S1 Differentially Expressed Genes in Col-0 compared with strigolactone mutants.

Table S2 Overlap of all differentially Expressed Genes in the strigolactone mutants *max4* (*more axillary growth4*), *max2* and *d14* (*dwarf14*).

Table S3 Differentially Expressed Genes in wild-type plants compared with *max2* (*more axillary growth2*) and trehalose 6-phosphate mutants.

Table S4 List of all primers used in this study.

Please note: Wiley is not responsible for the content or functionality of any Supporting Information supplied by the authors. Any queries (other than missing material) should be directed to the *New Phytologist* Central Office.